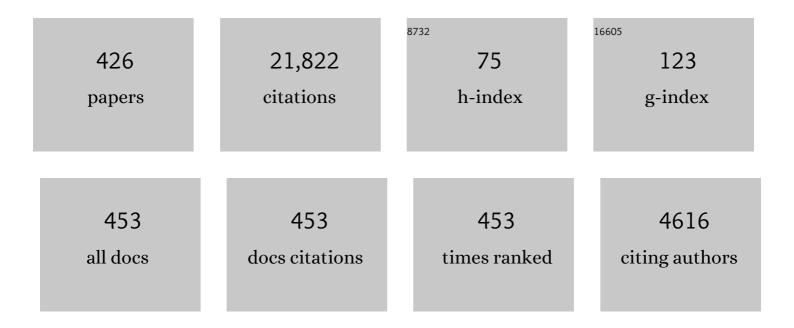
James A Slavin

List of Publications by Year in descending order

Source: https://exaly.com/author-pdf/6800922/publications.pdf Version: 2024-02-01



#	Article	IF	CITATIONS
1	The WIND magnetic field investigation. Space Science Reviews, 1995, 71, 207-229.	3.7	1,225
2	The Magnetospheric Multiscale Magnetometers. Space Science Reviews, 2016, 199, 189-256.	3.7	896
3	The MESSENGER mission to Mercury: scientific objectives and implementation. Planetary and Space Science, 2001, 49, 1445-1465.	0.9	361
4	The Global Magnetic Field of Mercury from MESSENGER Orbital Observations. Science, 2011, 333, 1859-1862.	6.0	301
5	An ISEE 3 study of average and substorm conditions in the distant magnetotail. Journal of Geophysical Research, 1985, 90, 10875-10895.	3.3	292
6	THE CLUSTER MAGNETIC FIELD INVESTIGATION. Space Science Reviews, 1997, 79, 65-91.	3.7	287
7	Geotail observations of magnetic flux ropes in the plasma sheet. Journal of Geophysical Research, 2003, 108, SMP 10-1.	3.3	285
8	Solar wind flow about the terrestrial planets 1. Modeling bow shock position and shape. Journal of Geophysical Research, 1981, 86, 11401-11418.	3.3	283
9	Structure of the magnetotail at 220 R _E and its response to geomagnetic activity. Geophysical Research Letters, 1984, 11, 5-7.	1.5	256
10	The Magnetometer Instrument on MESSENGER. Space Science Reviews, 2007, 131, 417-450.	3.7	254
11	Magnetic fields near Mars: first results. Nature, 1989, 341, 604-607.	13.7	246
12	MESSENGER Observations of Magnetic Reconnection in Mercury's Magnetosphere. Science, 2009, 324, 606-610.	6.0	234
13	Global simulation of the Geospace Environment Modeling substorm challenge event. Journal of Geophysical Research, 2001, 106, 381-395.	3.3	232
14	Three-dimensional position and shape of the bow shock and their variation with Alfvénic, sonic and magnetosonic Mach numbers and interplanetary magnetic field orientation. Journal of Geophysical Research, 1995, 100, 7907.	3.3	210
15	The Structure of Mercury's Magnetic Field from MESSENGER's First Flyby. Science, 2008, 321, 82-85.	6.0	194
16	Substorm associated traveling compression regions in the distant tail: Iseeâ€3 Geotail observations. Geophysical Research Letters, 1984, 11, 657-660.	1.5	190
17	Magnetic flux transfer associated with expansions and contractions of the dayside magnetosphere. Journal of Geophysical Research, 1978, 83, 3831-3839.	3.3	183
18	Mercury's magnetopause and bow shock from MESSENGER Magnetometer observations. Journal of Geophysical Research: Space Physics, 2013, 118, 2213-2227.	0.8	182

#	Article	lF	CITATIONS
19	MESSENGER Observations of Extreme Loading and Unloading of Mercury's Magnetic Tail. Science, 2010, 329, 665-668.	6.0	172
20	Observations of the dayside ionopause and ionosphere of Venus. Journal of Geophysical Research, 1980, 85, 7679-7696.	3.3	170
21	Return to Mercury: A Global Perspective on MESSENGER's First Mercury Flyby. Science, 2008, 321, 59-62.	6.0	170
22	Mercury's Magnetosphere After MESSENGER's First Flyby. Science, 2008, 321, 85-89.	6.0	166
23	Small-scale magnetic flux ropes in the solar wind. Geophysical Research Letters, 2000, 27, 57-60.	1.5	157
24	The effect of erosion on the solar wind standâ€off distance at Mercury. Journal of Geophysical Research, 1979, 84, 2076-2082.	3.3	156
25	Initial Pioneer Venus Magnetic Field Results: Dayside Observations. Science, 1979, 203, 745-748.	6.0	148
26	ISEE 3 observations of traveling compression regions in the Earth's magnetotail. Journal of Geophysical Research, 1993, 98, 15425-15446.	3.3	141
27	MESSENGER observations of magnetopause structure and dynamics at Mercury. Journal of Geophysical Research: Space Physics, 2013, 118, 997-1008.	0.8	141
28	Evidence for slowâ€mode shocks in the deep geomagnetic tail. Geophysical Research Letters, 1984, 11, 599-602.	1.5	134
29	Lowâ€degree structure in Mercury's planetary magnetic field. Journal of Geophysical Research, 2012, 117,	3.3	131
30	Bow Shock and Upstream Phenomena at Mars. Space Science Reviews, 2004, 111, 115-181.	3.7	129
31	Evolution of the Earth's distant magnetotail: ISEE 3 electron plasma results. Journal of Geophysical Research, 1984, 89, 11007-11012.	3.3	125
32	MESSENGER observations of Mercury's dayside magnetosphere under extreme solar wind conditions. Journal of Geophysical Research: Space Physics, 2014, 119, 8087-8116.	0.8	125
33	The distant magnetotail's response to a strong interplanetary magnetic field B _y : Twisting, flattening, and field line bending. Journal of Geophysical Research, 1985, 90, 4011-4019.	3.3	123
34	MESSENGER Observations of the Composition of Mercury's Ionized Exosphere and Plasma Environment. Science, 2008, 321, 90-92.	6.0	121
35	lo and its plasma environment. Journal of Geophysical Research, 1980, 85, 5959-5968.	3.3	119
36	Solar wind flow about the outer planets: Gas dynamic modeling of the Jupiter and Saturn bow shocks. Journal of Geophysical Research, 1985, 90, 6275-6286.	3.3	119

#	Article	IF	CITATIONS
37	Average plasma and magnetic field variations in the distant magnetotail associated with nearâ€Earth substorm effects. Journal of Geophysical Research, 1987, 92, 71-81.	3.3	119
38	Average configuration of the distant (<220 R _e) magnetotail: Initial ISEEâ€3 magnetic field results. Geophysical Research Letters, 1983, 10, 973-976.	1.5	117
39	Substorm energy budget during low and high solar activity: 1997 and 1999 compared. Journal of Geophysical Research, 2002, 107, SMP 15-1.	3.3	116
40	Transient and localized processes in the magnetotail: a review. Annales Geophysicae, 2008, 26, 955-1006.	0.6	112
41	Mercury's magnetospheric magnetic field after the first two MESSENGER flybys. Icarus, 2010, 209, 23-39.	1.1	110
42	MESSENGER observations of Mercury's magnetic field structure. Journal of Geophysical Research, 2012, 117, .	3.3	109
43	CDAW 8 observations of plasmoid signatures in the geomagnetic tail: An assessment. Journal of Geophysical Research, 1989, 94, 15153-15175.	3.3	108
44	Observations of multiple X-line structure in the Earth's magnetotail current sheet: A Cluster case study. Geophysical Research Letters, 2005, 32, .	1.5	108
45	Mercury's Weather-Beaten Surface: Understanding Mercury in the Context of Lunar and Asteroidal Space Weathering Studies. Space Science Reviews, 2014, 181, 121-214.	3.7	108
46	Timing accuracy for the simple planar propagation of magnetic field structures in the solar wind. Geophysical Research Letters, 1998, 25, 2509-2512.	1.5	107
47	MESSENGER Observations of the Spatial Distribution of Planetary Ions Near Mercury. Science, 2011, 333, 1862-1865.	6.0	102
48	Magnetotail flux ropes. Geophysical Research Letters, 1984, 11, 1090-1093.	1.5	99
49	Characterization of the IMF <i>B_y</i> â€dependent fieldâ€aligned currents in the cleft region based on DE 2 observations. Journal of Geophysical Research, 1993, 98, 1393-1407.	3.3	99
50	Magnetic flux pileup and plasma depletion in Mercury's subsolar magnetosheath. Journal of Geophysical Research: Space Physics, 2013, 118, 7181-7199.	0.8	96
51	The solar wind interaction with Venus: Pioneer Venus observations of bow shock location and structure. Journal of Geophysical Research, 1980, 85, 7625-7641.	3.3	95
52	Boundary layer formation in the magnetotail: Geotail observations and comparisons with a global MHD simulation. Geophysical Research Letters, 1997, 24, 951-954.	1.5	95
53	lonâ€scale secondary flux ropes generated by magnetopause reconnection as resolved by MMS. Geophysical Research Letters, 2016, 43, 4716-4724.	1.5	95
54	The Magnetic Field of Mercury. Space Science Reviews, 2010, 152, 307-339.	3.7	94

#	Article	IF	CITATIONS
55	Solar wind flow about the terrestrial planets: 2. Comparison with gas dynamic theory and implications for solarâ€planetary interactions. Journal of Geophysical Research, 1983, 88, 19-35.	3.3	92
56	A proxy for determining solar wind dynamic pressure at Mars using Mars Global Surveyor data. Journal of Geophysical Research, 2003, 108, .	3.3	92
57	Detailed examination of a plasmoid in the distant magnetotail with ISEE 3. Geophysical Research Letters, 1984, 11, 1046-1049.	1.5	91
58	A THEMIS survey of flux ropes and traveling compression regions: Location of the near-Earth reconnection site during solar minimum. Journal of Geophysical Research, 2011, 116, n/a-n/a.	3.3	91
59	Giacobiniâ€Zinner magnetotail: ICE magnetic field observations. Geophysical Research Letters, 1986, 13, 283-286.	1.5	90
60	The solar wind interaction with Mars: Mariner 4, Mars 2, Mars 3, Mars 5, and Phobos 2 observations of bow shock position and shape. Journal of Geophysical Research, 1991, 96, 11235-11241.	3.3	89
61	Global MHD simulations of Mercury's magnetosphere with coupled planetary interior: Induction effect of the planetary conducting core on the global interaction. Journal of Geophysical Research: Space Physics, 2015, 120, 4763-4775.	0.8	89
62	lonospheric current signatures of transient plasma sheet flows. Journal of Geophysical Research, 2000, 105, 10677-10690.	3.3	87
63	MESSENGER and Mariner 10 flyby observations of magnetotail structure and dynamics at Mercury. Journal of Geophysical Research, 2012, 117, .	3.3	86
64	Observations of Mercury's northern cusp region with MESSENGER's Magnetometer. Geophysical Research Letters, 2012, 39, .	1.5	86
65	MESSENGER observations of a fluxâ€transferâ€event shower at Mercury. Journal of Geophysical Research, 2012, 117, .	3.3	85
66	Distribution and compositional variations of plasma ions in Mercury's space environment: The first three Mercury years of MESSENGER observations. Journal of Geophysical Research: Space Physics, 2013, 118, 1604-1619.	0.8	85
67	Response of the magnetotail to changes in the open flux content of the magnetosphere. Journal of Geophysical Research, 2004, 109, .	3.3	83
68	Heavy ion mass loading of the geomagnetic field near the plasmapause and ULF wave implications. Geophysical Research Letters, 2005, 32, n/a-n/a.	1.5	83
69	Cluster observations of traveling compression regions in the near-tail. Journal of Geophysical Research, 2005, 110, .	3.3	79
70	Three-dimensional position and shape of the bow shock and their variation with upstream Mach numbers and interplanetary magnetic field orientation. Journal of Geophysical Research, 2005, 110, .	3.3	79
71	Structure and dynamics of Mercury's magnetospheric cusp: MESSENGER measurements of protons and planetary ions. Journal of Geophysical Research: Space Physics, 2014, 119, 6587-6602.	0.8	79
72	Energetic ion regimes in the deep geomagnetic tail: ISEEâ€3. Geophysical Research Letters, 1984, 11, 275-278.	1.5	78

#	Article	lF	CITATIONS
73	MESSENGER observations of the plasma environment near Mercury. Planetary and Space Science, 2011, 59, 2004-2015.	0.9	78
74	The solar wind interaction with Mars revisited. Journal of Geophysical Research, 1982, 87, 10285-10296.	3.3	77
75	Slow mode shocks in the Earth' magnetotail: ISEEâ€3. Geophysical Research Letters, 1984, 11, 1054-1057.	1.5	77
76	Cluster electric current density measurements within a magnetic flux rope in the plasma sheet. Geophysical Research Letters, 2003, 30, .	1.5	77
77	Limits on the possible intrinsic magnetic field of Venus. Journal of Geophysical Research, 1980, 85, 8319-8332.	3.3	73
78	Plasma wave spectra near slow mode shocks in the distant magnetotail. Geophysical Research Letters, 1984, 11, 1050-1053.	1.5	73
79	Planetary Mach cones: Theory and observation. Journal of Geophysical Research, 1984, 89, 2708-2714.	3.3	73
80	Cassini observations of plasmoid structure and dynamics: Implications for the role of magnetic reconnection in magnetospheric circulation at Saturn. Journal of Geophysical Research, 2011, 116, n/a-n/a.	3.3	73
81	MESSENGER observations of dipolarization events in Mercury's magnetotail. Journal of Geophysical Research, 2012, 117, .	3.3	72
82	Plasma entry into the distant tail lobes: ISEEâ€3. Geophysical Research Letters, 1984, 11, 1078-1081.	1.5	71
83	MESSENGER observations of flux ropes in Mercury's magnetotail. Planetary and Space Science, 2015, 115, 77-89.	0.9	71
84	Investigating Mercury's Environment with the Two-Spacecraft BepiColombo Mission. Space Science Reviews, 2020, 216, 1.	3.7	71
85	Magnetic structure of the distant geotail from â^'60 to â^'220 R _e : ISEEâ€3. Geophysical Research Letters, 1984, 11, 1-4.	1.5	69
86	MESSENGER orbital observations of largeâ€amplitude Kelvinâ€Helmholtz waves at Mercury's magnetopause. Journal of Geophysical Research, 2012, 117, .	3.3	69
87	Saturn's dynamic magnetotail: A comprehensive magnetic field and plasma survey of plasmoids and traveling compression regions and their role in global magnetospheric dynamics. Journal of Geophysical Research: Space Physics, 2014, 119, 5465-5494.	0.8	69
88	The interplanetary magnetic field during solar cycle 21: ISEEâ€3/ICE observations. Geophysical Research Letters, 1986, 13, 513-516.	1.5	67
89	Modeling of the magnetosphere of Mercury at the time of the first MESSENGER flyby. Icarus, 2010, 209, 3-10.	1.1	67
90	Mercury's magnetosphere–solar wind interaction for northward and southward interplanetary magnetic field: Hybrid simulation results. Icarus, 2010, 209, 11-22.	1.1	66

#	Article	IF	CITATIONS
91	Correlation between magnetic and electric field perturbations in the fieldâ€aligned current regions deduced from DE 2 observations. Journal of Geophysical Research, 1992, 97, 13877-13887.	3.3	65
92	Equatorial bubbles updrafting at supersonic speeds. Journal of Geophysical Research, 1992, 97, 8581-8590.	3.3	65
93	ISEE 3 observations of plasmoids with flux rope magnectic topologies. Geophysical Research Letters, 1995, 22, 2061-2064.	1.5	65
94	Simultaneous observations of earthward flow bursts and plasmoid ejection during magnetospheric substorms. Journal of Geophysical Research, 2002, 107, SMP 13-1.	3.3	65
95	Cometâ€solar wind interaction: Dynamical length scales and models. Geophysical Research Letters, 1986, 13, 239-242.	1.5	64
96	ISEE 3 plasmoid and TCR observations during an extended interval of substorm activity. Geophysical Research Letters, 1992, 19, 825-828.	1.5	63
97	Structure of the magnetic pileup boundary at Mars and Venus. Journal of Geophysical Research, 2005, 110, .	3.3	63
98	Average motion, structure and orientation of the distant magnetotail determined from remote sensing of the edge of the plasma sheet boundary layer withE> 35 keV ions. Journal of Geophysical Research, 1995, 100, 185.	3.3	62
99	Global Threeâ€Dimensional Simulation of Earth's Dayside Reconnection Using a Twoâ€Way Coupled Magnetohydrodynamics With Embedded Particleâ€inâ€Cell Model: Initial Results. Journal of Geophysical Research: Space Physics, 2017, 122, 10,318.	0.8	62
100	The lunar wake at 6.8 RL: WIND magnetic field observations. Geophysical Research Letters, 1996, 23, 1263-1266.	1.5	61
101	Determination of the properties of Mercury's magnetic field by the MESSENGER mission. Planetary and Space Science, 2004, 52, 733-746.	0.9	61
102	Magnetospheric substorms are strongly modulated by interplanetary high-speed streams. Geophysical Research Letters, 2005, 32, .	1.5	61
103	Shocks and Storm Sudden Commencements. Astrophysics and Space Science Library, 1986, , 345-365.	1.0	60
104	Pioneer Venus Orbiter magnetic field and plasma observations in the Venus magnetotail. Journal of Geophysical Research, 1989, 94, 2383-2398.	3.3	59
105	Paraboloid model of Mercury's magnetosphere. Journal of Geophysical Research, 2008, 113, .	3.3	59
106	A correlative study of magnetic flux transfer in the magnetosphere. Journal of Geophysical Research, 1979, 84, 2573-2578.	3.3	58
107	MESSENGER observations of large flux transfer events at Mercury. Geophysical Research Letters, 2010, 37, .	1.5	57
108	Initial Pioneer Venus Magnetic Field Results: Nightside Observations. Science, 1979, 205, 114-116.	6.0	56

#	Article	IF	CITATIONS
109	Loading-unloading processes in the nightside ionosphere. Geophysical Research Letters, 2000, 27, 1627-1630.	1.5	55
110	MESSENGER: Exploring Mercury's Magnetosphere. Space Science Reviews, 2007, 131, 133-160.	3.7	55
111	Temporal and spatial characteristics of Pc1 waves observed by ST5. Journal of Geophysical Research, 2008, 113, .	3.3	55
112	MESSENGER observations of Mercury's magnetosphere during northward IMF. Geophysical Research Letters, 2009, 36, .	1.5	55
113	Steadyâ€state fieldâ€aligned currents at Mercury. Geophysical Research Letters, 2014, 41, 7444-7452.	1.5	55
114	Spatial distribution of Mercury's flux ropes and reconnection fronts: MESSENGER observations. Journal of Geophysical Research: Space Physics, 2016, 121, 7590-7607.	0.8	55
115	An evaluation of three predictors of geomagnetic activity. Journal of Geophysical Research, 1982, 87, 2558-2562.	3.3	54
116	Characteristics of the terrestrial field-aligned current system. Annales Geophysicae, 2011, 29, 1713-1729.	0.6	54
117	Structure and statistical properties of plasmoids in Jupiter's magnetotail. Journal of Geophysical Research: Space Physics, 2014, 119, 821-843.	0.8	54
118	MESSENGER observations of large dayside flux transfer events: Do they drive Mercury's substorm cycle?. Journal of Geophysical Research: Space Physics, 2014, 119, 5613-5623.	0.8	54
119	The Earth: Plasma Sources, Losses, and Transport Processes. Space Science Reviews, 2015, 192, 145-208.	3.7	54
120	Major flattening of the distant geomagnetic tail. Journal of Geophysical Research, 1986, 91, 4223-4237.	3.3	53
121	The effects of neutral inertia on ionospheric currents in the highâ€latitude thermosphere following a geomagnetic storm. Journal of Geophysical Research, 1993, 98, 7775-7790.	3.3	53
122	Global configuration of the magnetotail current sheet as derived from Geotail, Wind, IMP 8 and ISEE 1/2 data. Journal of Geophysical Research, 1998, 103, 6827-6841.	3.3	53
123	Mercury's crossâ€ŧail current sheet: Structure, Xâ€ŀine location and stress balance. Geophysical Research Letters, 2017, 44, 678-686.	1.5	53
124	MESSENGER Observations of Disappearing Dayside Magnetosphere Events at Mercury. Journal of Geophysical Research: Space Physics, 2019, 124, 6613-6635.	0.8	53
125	Large scale temporal and radial gradients in the IMF: Helios 1, 2, ISEEâ€3, and Pioneer 10, 11. Geophysical Research Letters, 1984, 11, 279-282.	1.5	52
126	Sources of sodium in the lunar exosphere: Modeling using ground-based observations of sodium emission and spacecraft data of the plasma. Icarus, 2010, 205, 364-374.	1.1	52

#	Article	IF	CITATIONS
127	Magnetospheres of the Galilean Satellites. Science, 1979, 205, 491-493.	6.0	51
128	An empirical model of Saturn's bow shock: Cassini observations of shock location and shape. Journal of Geophysical Research, 2008, 113, .	3.3	51
129	Observations of Kelvinâ€Helmholtz waves along the duskâ€side boundary of Mercury's magnetosphere during MESSENGER's third flyby. Geophysical Research Letters, 2010, 37, .	1.5	50
130	lon kinetic properties in Mercury's preâ€midnight plasma sheet. Geophysical Research Letters, 2014, 41, 5740-5747.	1.5	50
131	MESSENGER observations of magnetospheric substorm activity in Mercury's near magnetotail. Geophysical Research Letters, 2015, 42, 3692-3699.	1.5	50
132	Multispacecraft analysis of dipolarization fronts and associated whistler wave emissions using MMS data. Geophysical Research Letters, 2016, 43, 7279-7286.	1.5	49
133	MESSENGER Observations and Global Simulations of Highly Compressed Magnetosphere Events at Mercury. Journal of Geophysical Research: Space Physics, 2019, 124, 229-247.	0.8	49
134	Hermean Magnetosphere-Solar Wind Interaction. Space Science Reviews, 2007, 132, 529-550.	3.7	48
135	Mercury's threeâ€dimensional asymmetric magnetopause. Journal of Geophysical Research: Space Physics, 2015, 120, 7658-7671.	0.8	48
136	Analysis of the 3-D shape of the terrestrial bow shock by interball/magion 4 observations. Advances in Space Research, 2001, 28, 857-862.	1.2	47
137	ARTEMIS Science Objectives. Space Science Reviews, 2011, 165, 59-91.	3.7	47
138	A strong dawn/dusk asymmetry in Pc5 pulsation occurrence observed by the DE-1 satellite. Geophysical Research Letters, 1995, 22, 2053-2056.	1.5	46
139	Solar wind forcing at Mercury: WSAâ€ENLIL model results. Journal of Geophysical Research: Space Physics, 2013, 118, 45-57.	0.8	46
140	Plasma distribution in Mercury's magnetosphere derived from MESSENGER Magnetometer and Fast Imaging Plasma Spectrometer observations. Journal of Geophysical Research: Space Physics, 2014, 119, 2917-2932.	0.8	46
141	WIND, GEOTAIL, and GOES 9 observations of magnetic field dipolarization and bursty bulk flows in the near-tail. Geophysical Research Letters, 1997, 24, 971-974.	1.5	45
142	The BepiColombo Planetary Magnetometer MPO-MAG: What Can We Learn from the Hermean Magnetic Field?. Space Science Reviews, 2021, 217, 1.	3.7	45
143	Coupling between the solar wind and the magnetosphere: CDAW 6. Journal of Geophysical Research, 1985, 90, 1191-1199.	3.3	44
144	ISEE 3 observations during the CDAW 8 intervals: Case studies of the distant geomagnetic tail covering a wide range of geomagnetic activity. Journal of Geophysical Research, 1989, 94, 15189-15220.	3.3	44

#	Article	IF	CITATIONS
145	Influence of plasma ions on source rates for the lunar exosphere during passage through the Earth's magnetosphere. Geophysical Research Letters, 2008, 35, .	1.5	44
146	Global Tenâ€Moment Multifluid Simulations of the Solar Wind Interaction with Mercury: From the Planetary Conducting Core to the Dynamic Magnetosphere. Geophysical Research Letters, 2019, 46, 11584-11596.	1.5	44
147	Strong electron bidirectional anisotropies in the distant tail: ISEE 3 observations of polar rain. Journal of Geophysical Research, 1986, 91, 5637-5662.	3.3	43
148	A three dimensional gasdynamic model for solar wind flow past nonaxisymmetric magnetospheres: Application to Jupiter and Saturn. Journal of Geophysical Research, 1989, 94, 13353-13365.	3.3	43
149	Field-aligned Poynting Flux observations in the high-latitude ionosphere. Journal of Geophysical Research, 1994, 99, 11417.	3.3	43
150	Magnetospheric current systems during stormtime sawtooth events. Journal of Geophysical Research, 2006, 111, .	3.3	43
151	From space weather toward space climate time scales: Substorm analysis from 1993 to 2008. Journal of Geophysical Research, 2011, 116, .	3.3	43
152	Clobal observations of magnetospheric highâ€ <i>m</i> poloidal waves during the 22 June 2015 magnetic storm. Geophysical Research Letters, 2017, 44, 3456-3464.	1.5	43
153	Observations of large scale steady magnetic fields in the nightside Venus ionosphere and near wake. Geophysical Research Letters, 1981, 8, 517-520.	1.5	42
154	Observations of the flank of Earth's bow shock to â^'110 R _E by ISEE 3/ICE. Geophysical Research Letters, 1990, 17, 753-756.	1.5	41
155	Wind observations of the terrestrial bow shock: 3-D shape and motion. Earth, Planets and Space, 2001, 53, 1001-1009.	0.9	41
156	Large-Scale Structure and Dynamics of the Magnetotails of Mercury, Earth, Jupiter and Saturn. Space Science Reviews, 2014, 182, 85-154.	3.7	41
157	Spatial gradients in the heliospheric magnetic field: Pioneer 11 observations between 1 AU and 24 AU, and over solar cycle 21. Journal of Geophysical Research, 1990, 95, 1-11.	3.3	40
158	Space Technology 5 multiâ€point measurements of nearâ€Earth magnetic fields: Initial results. Geophysical Research Letters, 2008, 35, .	1.5	40
159	Quasi-trapped ion and electron populations at Mercury. Geophysical Research Letters, 2011, 38, n/a-n/a.	1.5	40
160	Upstream ultraâ€low frequency waves in Mercury's foreshock region: MESSENGER magnetic field observations. Journal of Geophysical Research: Space Physics, 2013, 118, 2809-2823.	0.8	40
161	MESSENGER observations of multiscale Kelvinâ€Helmholtz vortices at Mercury. Journal of Geophysical Research: Space Physics, 2015, 120, 4354-4368.	0.8	40
162	Ground-based studies of ionospheric convection associated with substorm expansion. Journal of Geophysical Research, 1994, 99, 19451.	3.3	39

#	Article	IF	CITATIONS
163	Multispacecraft observations of sudden impulses in the magnetotail caused by solar wind pressure discontinuities: Wind and IMP 8. Journal of Geophysical Research, 1998, 103, 17293-17305.	3.3	39
164	Kinetic-scale magnetic turbulence and finite Larmor radius effects at Mercury. Journal of Geophysical Research, 2011, 116, n/a-n/a.	3.3	39
165	Survey of coherent â^¼1 Hz waves in Mercury's inner magnetosphere from MESSENGER observations. Journal of Geophysical Research, 2012, 117, .	3.3	39
166	Mercury's surface magnetic field determined from protonâ€reflection magnetometry. Geophysical Research Letters, 2014, 41, 4463-4470.	1.5	39
167	Plasma Sources in Planetary Magnetospheres: Mercury. Space Science Reviews, 2015, 192, 91-144.	3.7	39
168	Interplanetary magnetic field properties and variability near Mercury's orbit. Journal of Geophysical Research: Space Physics, 2017, 122, 7907-7924.	0.8	39
169	MMS Examination of FTEs at the Earth's Subsolar Magnetopause. Journal of Geophysical Research: Space Physics, 2018, 123, 1224-1241.	0.8	39
170	Position and shape of the Venus bow shock: Pioneer Venus Orbiter observations. Geophysical Research Letters, 1979, 6, 901-904.	1.5	38
171	Plasmasheet magnetic fields in the distant tail. Geophysical Research Letters, 1984, 11, 1062-1065.	1.5	38
172	Magnetic field properties of the distant magnetotail magnetopause and boundary layer. Journal of Geophysical Research, 1985, 90, 9561-9575.	3.3	38
173	Kinetic instabilities in Mercury's magnetosphere: Threeâ€dimensional simulation results. Geophysical Research Letters, 2009, 36, .	1.5	38
174	Plasma pressure in Mercury's equatorial magnetosphere derived from MESSENGER Magnetometer observations. Geophysical Research Letters, 2011, 38, n/a-n/a.	1.5	38
175	Flux transfer event observation at Saturn's dayside magnetopause by the Cassini spacecraft. Geophysical Research Letters, 2016, 43, 6713-6723.	1.5	38
176	MESSENGER Observations of Magnetotail Loading and Unloading: Implications for Substorms at Mercury. Journal of Geophysical Research: Space Physics, 2017, 122, 11,402.	0.8	38
177	MESSENGER and Venus Express observations of the solar wind interaction with Venus. Geophysical Research Letters, 2009, 36, .	1.5	37
178	Space environment of Mercury at the time of the first MESSENGER flyby: Solar wind and interplanetary magnetic field modeling of upstream conditions. Journal of Geophysical Research, 2009, 114, .	3.3	37
179	A comparative study of dipolarization fronts at MMS and Cluster. Geophysical Research Letters, 2016, 43, 6012-6019.	1.5	37
180	ISTP observations of plasmoid ejection: IMP 8 and Geotail. Journal of Geophysical Research, 1998, 103, 119-133.	3.3	36

#	Article	IF	CITATIONS
181	Limits to Mercury's magnesium exosphere from MESSENGER second flyby observations. Planetary and Space Science, 2011, 59, 1992-2003.	0.9	36
182	Compressibility of Mercury's dayside magnetosphere. Geophysical Research Letters, 2015, 42, 10,135.	1.5	36
183	Magnetopause erosion during the 17 March 2015 magnetic storm: Combined fieldâ€aligned currents, auroral oval, and magnetopause observations. Geophysical Research Letters, 2016, 43, 2396-2404.	1.5	36
184	Energetic Electron Acceleration and Injection During Dipolarization Events in Mercury's Magnetotail. Journal of Geophysical Research: Space Physics, 2017, 122, 12,170.	0.8	36
185	A Pioneerâ€Voyager study of the solar wind interaction with Saturn. Geophysical Research Letters, 1983, 10, 9-12.	1.5	35
186	IMPâ€8 observations of traveling compression regions: New evidence for nearâ€Earth plasmoids and neutral lines. Geophysical Research Letters, 1990, 17, 913-916.	1.5	35
187	Satellite measurements through the center of a substorm surge. Journal of Geophysical Research, 1994, 99, 23639.	3.3	35
188	The interplanetary magnetic field environment at Mercury's orbit. Planetary and Space Science, 2011, 59, 2075-2085.	0.9	35
189	MESSENGER Observations of Transient Bursts of Energetic Electrons in Mercury's Magnetosphere. Science, 2011, 333, 1865-1868.	6.0	35
190	Hot flow anomalies at Venus. Journal of Geophysical Research, 2012, 117, .	3.3	35
191	Cassini in situ observations of long-duration magnetic reconnection in Saturn's magnetotail. Nature Physics, 2016, 12, 268-271.	6.5	35
192	The bow wave of comet Giacobiniâ€Zinner: Ice magnetic field observations. Geophysical Research Letters, 1986, 13, 243-246.	1.5	34
193	Mirror mode structures and ELF plasma waves in the Giacobini-Zinner magnetosheath. Nonlinear Processes in Geophysics, 1999, 6, 229-234.	0.6	34
194	Planetary bow shocks: Gasdynamic analytic approach. Journal of Geophysical Research, 2003, 108, .	3.3	34
195	RADIAL EVOLUTION OF A MAGNETIC CLOUD: <i>MESSENGER</i> , <i>STEREO</i> , AND <i>VENUS EXPRESS</i> OBSERVATIONS. Astrophysical Journal, 2015, 807, 177.	1.6	34
196	Threeâ€Dimensional Magnetic Reconnection With a Spatially Confined Xâ€Line Extent: Implications for Dipolarizing Flux Bundles and the Dawnâ€Dusk Asymmetry. Journal of Geophysical Research: Space Physics, 2019, 124, 2819-2830.	0.8	34
197	Interaction of the solar wind with the planet Mars: Phobos 2 magnetic field observations. Planetary and Space Science, 1991, 39, 75-81.	0.9	33
198	Cluster four spacecraft measurements of small traveling compression regions in the near-tail. Geophysical Research Letters, 2003, 30, n/a-n/a.	1.5	33

#	Article	IF	CITATIONS
199	Transition from substorm growth to substorm expansion phase as observed with a radial configuration of ISTP and Cluster spacecraft. Annales Geophysicae, 2005, 23, 2183-2198.	0.6	33
200	Cluster observations of flux rope structures in the near-tail. Annales Geophysicae, 2006, 24, 651-666.	0.6	33
201	In situ observations of the effect of a solar wind compression on Saturn's magnetotail. Journal of Geophysical Research, 2010, 115, .	3.3	33
202	The dayside magnetospheric boundary layer at Mercury. Planetary and Space Science, 2011, 59, 2037-2050.	0.9	33
203	MHD simulations of the transition of magnetic reconnection from closed to open field lines. Journal of Geophysical Research, 1996, 101, 10805-10816.	3.3	32
204	Cluster observations of sudden impulses in the magnetotail caused by interplanetary shocks and pressure increases. Annales Geophysicae, 2005, 23, 609-624.	0.6	32
205	Multiscale Currents Observed by MMS in the Flow Braking Region. Journal of Geophysical Research: Space Physics, 2018, 123, 1260-1278.	0.8	32
206	Postoperative metabolic patterns following immediate total nutritional support: Hormone levels, DNA synthesis, nitrogen balance, and accelerated wound healing. Journal of Surgical Research, 1976, 21, 383-393.	0.8	31
207	Auroral ionospheric signatures of the plasma sheet boundary layer in the evening sector. Journal of Geophysical Research, 1994, 99, 2489.	3.3	31
208	Planetary bow shocks: Asymptotic MHD Mach cones. Earth, Planets and Space, 2003, 55, 33-38.	0.9	31
209	Observations of suprathermal electrons in Mercury's magnetosphere during the three MESSENGER flybys. Planetary and Space Science, 2011, 59, 2016-2025.	0.9	31
210	Intense energetic electron flux enhancements in Mercury's magnetosphere: An integrated view with highâ€resolution observations from MESSENGER. Journal of Geophysical Research: Space Physics, 2016, 121, 2171-2184.	0.8	31
211	The Magnetic Field Structure of Mercury's Magnetotail. Journal of Geophysical Research: Space Physics, 2018, 123, 548-566.	0.8	31
212	A comparison of Pioneer Venus and Venera bow shock observations: Evidence for a solar cycle variation. Geophysical Research Letters, 1979, 6, 905-908.	1.5	30
213	Quantitative model of the Martian magnetopause shape and its variation with the solar wind ram pressure based on Phobos 2 observations. Journal of Geophysical Research, 1997, 102, 2147-2155.	3.3	30
214	Nano/Micro Satellite Constellations for Earth and Space Science. Acta Astronautica, 2003, 52, 785-791.	1.7	30
215	Magnetotail response to prolonged southward IMFBzintervals: Loading, unloading, and continuous magnetospheric dissipation. Journal of Geophysical Research, 2005, 110, .	3.3	30
216	Electron transport and precipitation at Mercury during the MESSENGER flybys: Implications for electron-stimulated desorption. Planetary and Space Science, 2011, 59, 2026-2036.	0.9	30

#	Article	IF	CITATIONS
217	Transient, smallâ€scale fieldâ€aligned currents in the plasma sheet boundary layer during storm time substorms. Geophysical Research Letters, 2016, 43, 4841-4849.	1.5	30
218	MMS Study of the Structure of Ion‣cale Flux Ropes in the Earth's Crossâ€Tail Current Sheet. Geophysical Research Letters, 2019, 46, 6168-6177.	1.5	30
219	The location of the dayside ionopause of Venus: Pioneer Venus Orbiter Magnetometer observations. Geophysical Research Letters, 1980, 7, 561-564.	1.5	29
220	Direct observations of passages of the distant neutral line (80â€140 R _E) following substorm pnsets: ISEEâ€3. Geophysical Research Letters, 1984, 11, 1042-1045.	1.5	29
221	Near-simultaneous bow shock crossings by WIND and IMP 8 on December 1, 1994. Geophysical Research Letters, 1996, 23, 1207-1210.	1.5	29
222	Magnetic field draping enhancement at Venus: Evidence for a magnetic pileup boundary. Geophysical Research Letters, 2003, 30, n/a-n/a.	1.5	29
223	Flux estimates of ions from the lunar exosphere. Geophysical Research Letters, 2012, 39, .	1.5	29
224	First observations of Mercury's plasma mantle by MESSENGER. Geophysical Research Letters, 2015, 42, 9666-9675.	1.5	29
225	MESSENGER observations of cusp plasma filaments at Mercury. Journal of Geophysical Research: Space Physics, 2016, 121, 8260-8285.	0.8	29
226	Coupling between Mercury and its nightside magnetosphere: Crossâ€ŧail current sheet asymmetry and substorm current wedge formation. Journal of Geophysical Research: Space Physics, 2017, 122, 8419-8433.	0.8	29
227	Statics and dynamics of Giacobiniâ€Zinner magnetic tail. Geophysical Research Letters, 1986, 13, 287-290.	1.5	28
228	Electron precipitation accompanying Pc 5 pulsations observed by the DE satellites and at a ground station. Journal of Geophysical Research, 1998, 103, 17587-17604.	3.3	28
229	The space environment of Mercury at the times of the second and third MESSENGER flybys. Planetary and Space Science, 2011, 59, 2066-2074.	0.9	28
230	Spatial distribution and spectral characteristics of energetic electrons in Mercury's magnetosphere. Journal of Geophysical Research, 2012, 117, .	3.3	28
231	A comparative study of distant magnetotail structure at Venus and Earth. Geophysical Research Letters, 1984, 11, 1074-1077.	1.5	27
232	Earthward flowing plasmoid: Structure and its related ionospheric signature. Journal of Geophysical Research, 2007, 112, .	3.3	27
233	Force balance at the magnetopause determined with MMS: Application to flux transfer events. Geophysical Research Letters, 2016, 43, 11,941.	1.5	27
234	MESSENGER observations of the energization and heating of protons in the nearâ€Mercury magnetotail. Geophysical Research Letters, 2017, 44, 8149-8158.	1.5	27

#	Article	IF	CITATIONS
235	Study of the solar wind deceleration upstream of the Martian terminator bow shock. Journal of Geophysical Research, 1997, 102, 2165-2173.	3.3	26
236	Longitudinal association between magnetotail reconnection and auroral breakup based on Geotail and Polar observations. Journal of Geophysical Research, 2008, 113, .	3.3	26
237	Narrowâ€band ultraâ€lowâ€frequency wave observations by MESSENGER during its January 2008 flyby through Mercury's magnetosphere. Geophysical Research Letters, 2009, 36, .	1.5	26
238	Sodiumâ€ion pickup observed above the magnetopause during MESSENGER's first Mercury flyby: Constraints on neutral exospheric models. Geophysical Research Letters, 2009, 36, .	1.5	26
239	Evidence for extended acceleration of solar flare ions from 1–8 MeV solar neutrons detected with the MESSENGER Neutron Spectrometer. Journal of Geophysical Research, 2010, 115, .	3.3	26
240	Studying Dawnâ€Ðusk Asymmetries of Mercury's Magnetotail Using MHDâ€EPIC Simulations. Journal of Geophysical Research: Space Physics, 2019, 124, 8954-8973.	0.8	26
241	SERENA: Particle Instrument Suite for Determining the Sun-Mercury Interaction from BepiColombo. Space Science Reviews, 2021, 217, 11.	3.7	26
242	Spatial extent and dynamics of a thin current sheet during the substorm growth phase on December 10, 1996. Journal of Geophysical Research, 1999, 104, 28475-28490.	3.3	25
243	Cyclic reformation of a quasiâ€parallel bow shock at Mercury: MESSENGER observations. Journal of Geophysical Research: Space Physics, 2013, 118, 6457-6464.	0.8	25
244	Isolated magnetic field structures in Mercury's magnetosheath as possible analogues for terrestrial magnetosheath plasmoids and jets. Planetary and Space Science, 2016, 129, 61-73.	0.9	25
245	Mercury's Solar Wind Interaction as Characterized by Magnetospheric Plasma Mantle Observations With MESSENGER. Journal of Geophysical Research: Space Physics, 2017, 122, 12,153.	0.8	25
246	BepiColombo Science Investigations During Cruise and Flybys at the Earth, Venus and Mercury. Space Science Reviews, 2021, 217, 1.	3.7	25
247	Pioneer magnetometer observations of the Venus bow shock. Nature, 1979, 282, 815-816.	13.7	24
248	By-controlled convection and field-aligned currents near midnight auroral oval for northward interplanetary magnetic field. Journal of Geophysical Research, 1994, 99, 6027.	3.3	24
249	Dual spacecraft observations of lobe magnetic field perturbations before, during and after plasmoid release. Geophysical Research Letters, 1999, 26, 2897-2900.	1.5	24
250	Space Technology 5 observations of the imbalance of regions 1 and 2 fieldâ€aligned currents and its implication to the crossâ€polar cap Pedersen currents. Journal of Geophysical Research, 2010, 115, .	3.3	24
251	Reconstruction of propagating Kelvin–Helmholtz vortices at Mercury's magnetopause. Planetary and Space Science, 2011, 59, 2051-2057.	0.9	24
252	Magnetotails at unmagnetized bodies: Comparison of comet Giacobiniâ€Zinner and Venus. Journal of Geophysical Research, 1987, 92, 10111-10117.	3.3	23

#	Article	IF	CITATIONS
253	"Substorms, plasmoids, flux ropes, and magnetotail flux loss on March 25, 1983: CDAW 8"". Journal of Geophysical Research, 1989, 94, 15135-15152.	3.3	23
254	Characteristics of the plasma distribution in Mercury's equatorial magnetosphere derived from MESSENGER Magnetometer observations. Journal of Geophysical Research, 2012, 117, .	3.3	23
255	Flux ropes in the Hermean magnetotail: Distribution, properties, and formation. Journal of Geophysical Research: Space Physics, 2017, 122, 8136-8153.	0.8	23
256	Flux Transfer Event Showers at Mercury: Dependence on Plasma <i>β</i> and Magnetic Shear and Their Contribution to the Dungey Cycle. Geophysical Research Letters, 2020, 47, e2020GL089784.	1.5	23
257	ISEE 3 magnetic field observations in the mgnetotail: Implications for reconnection. Geophysical Monograph Series, 1984, , 240-248.	0.1	22
258	The structure of a cometary Type I tail: Groundâ€based and ice observations of P/Giacobiniâ€Zinner. Geophysical Research Letters, 1986, 13, 1085-1088.	1.5	22
259	Active current sheets and candidate hot flow anomalies upstream of Mercury's bow shock. Journal of Geophysical Research: Space Physics, 2014, 119, 853-876.	0.8	22
260	Optimized merging of search coil and fluxgate data for MMS. Geoscientific Instrumentation, Methods and Data Systems, 2016, 5, 521-530.	0.6	22
261	Plasma Sheet Pressure Variations in the Nearâ€Earth Magnetotail During Substorm Growth Phase: THEMIS Observations. Journal of Geophysical Research: Space Physics, 2017, 122, 12,212.	0.8	22
262	MESSENGER Observations of Fast Plasma Flows in Mercury's Magnetotail. Geophysical Research Letters, 2018, 45, 10,110.	1.5	22
263	MMS Observations of Plasma Heating Associated With FTE Growth. Geophysical Research Letters, 2019, 46, 12654-12664.	1.5	22
264	Analysis of Magnetotail Flux Ropes with Strong Core Fields: ISEE 3 Observations. Journal of Geomagnetism and Geoelectricity, 1996, 48, 589-601.	0.8	22
265	Enhancements of energetic ions associated with travelling compression regions in the deep geomagnetic tail. Journal of Geophysical Research, 1987, 92, 64-70.	3.3	21
266	Magnetic field gradients from the STâ€5 constellation: Improving magnetic and thermal models of the lithosphere. Geophysical Research Letters, 2007, 34, .	1.5	21
267	A survey of hot flow anomalies at Venus. Journal of Geophysical Research: Space Physics, 2014, 119, 978-991.	0.8	21
268	Interpreting ~1 Hz magnetic compressional waves in Mercury's inner magnetosphere in terms of propagating ionâ€Bernstein waves. Journal of Geophysical Research: Space Physics, 2015, 120, 4213-4228.	0.8	21
269	Radial and latitudinal gradients in the interplanetary magnetic field: Evidence for meridional flux transport. Journal of Geophysical Research, 1986, 91, 6760-6764.	3.3	20
270	Particle acceleration and wave emissions associated with the formation of auroral cavities and enhancements. Journal of Geophysical Research, 1988, 93, 14567-14590.	3.3	20

#	Article	IF	CITATIONS
271	Analysis of an extended period of earthward plasma sheet flow at â^¼220 <i>R_E</i> : CDAW 8. Journal of Geophysical Research, 1989, 94, 15177-15188.	3.3	20
272	Simultaneous observations of subauroral electron temperature enhancements and electromagnetic ion cyclotron waves. Geophysical Research Letters, 1993, 20, 1723-1726.	1.5	20
273	On the determination of the Hermaean magnetic moment: A critical review. Physics of the Earth and Planetary Interiors, 1979, 20, 231-236.	0.7	19
274	A quantitative model of geomagnetic activity. Journal of Geophysical Research, 1982, 87, 9054-9058.	3.3	19
275	Search for pickâ€up ion generated Na ⁺ cyclotron waves at Mercury. Geophysical Research Letters, 2007, 34, .	1.5	19
276	On the possible formation of Alfvén wings at Mercury during encounters with coronal mass ejections. Geophysical Research Letters, 2009, 36, .	1.5	19
277	MESSENGER observations of Alfvénic and compressional waves during Mercury's substorms. Geophysical Research Letters, 2015, 42, 6189-6198.	1.5	19
278	Particles and Photons as Drivers for Particle Release from the Surfaces of the Moon and Mercury. Space Science Reviews, 2022, 218, 1.	3.7	19
279	Review of Mercury's dynamic magnetosphere: Post-MESSENGER era and comparative magnetospheres. Science China Earth Sciences, 2022, 65, 25-74.	2.3	19
280	The Giacobiniâ€Zinner magnetotail: Tail configuration and current sheet. Journal of Geophysical Research, 1987, 92, 1139-1152.	3.3	18
281	Viscously driven plasma flows in the deep geomagnetic tail. Geophysical Research Letters, 1992, 19, 1443-1446.	1.5	18
282	Traveling compression regions in the midtail: Fifteen years of IMP 8 observations. Journal of Geophysical Research, 1998, 103, 17641-17650.	3.3	18
283	Reconnection remnants in the magnetic cloud of October 18-19, 1995: A shock, monochromatic wave, heat flux dropout, and energetic ion beam. Journal of Geophysical Research, 2001, 106, 15985-16000.	3.3	18
284	Observations of a unique type of ULF wave by low-altitude Space Technology 5 satellites. Journal of Geophysical Research, 2011, 116, n/a-n/a.	3.3	18
285	Comparative Analysis of the Vlasiator Simulations and MMS Observations of Multiple Xâ€Line Reconnection and Flux Transfer Events. Journal of Geophysical Research: Space Physics, 2020, 125, e2019JA027410.	0.8	18
286	Multiâ€Fluid MHD Simulations of Europa's Plasma Interaction Under Different Magnetospheric Conditions. Journal of Geophysical Research: Space Physics, 2021, 126, e2020JA028888.	0.8	18
287	Planetary magnetospheres. Reviews of Geophysics, 1979, 17, 1677-1693.	9.0	17
288	Cluster electron observations of the separatrix layer during traveling compression regions. Geophysical Research Letters, 2005, 32, .	1.5	17

#	Article	IF	CITATIONS
289	Comparison of ultraâ€lowâ€frequency waves at Mercury under northward and southward IMF. Geophysical Research Letters, 2009, 36, .	1.5	17
290	A comparison of magnetic overshoots at the bow shocks of Mercury and Saturn. Journal of Geophysical Research: Space Physics, 2013, 118, 4381-4390.	0.8	17
291	MMS Multiâ€Point Analysis of FTE Evolution: Physical Characteristics and Dynamics. Journal of Geophysical Research: Space Physics, 2019, 124, 5376-5395.	0.8	17
292	Twisting of the Geomagnetic Tail. Astrophysics and Space Science Library, 1986, , 731-738.	1.0	17
293	THE MAGNETOSPHERE OF MERCURY. , 1989, , 514-561.		17
294	Cluster encounter with an energetic electron beam during a substorm. Journal of Geophysical Research, 2006, 111, .	3.3	16
295	Improving solar wind modeling at Mercury: Incorporating transient solar phenomena into the WSAâ€ENLIL model with the Cone extension. Journal of Geophysical Research: Space Physics, 2015, 120, 5667-5685.	0.8	16
296	MESSENGER observations of solar energetic electrons within Mercury's magnetosphere. Journal of Geophysical Research: Space Physics, 2015, 120, 8559-8571.	0.8	16
297	A Review of General Physical and Chemical Processes Related to Plasma Sources and Losses for Solar System Magnetospheres. Space Science Reviews, 2015, 192, 27-89.	3.7	16
298	lon cyclotron waves near <i>L</i> = 4.6: A groundâ€satellite correlation study. Journal of Geophysical Research, 1991, 96, 1451-1466.	3.3	15
299	IMP 8 observations of traveling compression regions in the mid-tail near substorm expansion phase onset. Geophysical Research Letters, 1997, 24, 353-356.	1.5	15
300	Solar wind-magnetosphere coupling during an isolated substorm event: A multispacecraft ISTP study. Geophysical Research Letters, 1997, 24, 983-986.	1.5	15
301	Statistical and superposed epoch study of dipolarization events using data from Wind perigee passes. Annales Geophysicae, 2005, 23, 831-851.	0.6	15
302	Space Technology 5 multipoint observations of temporal and spatial variability of fieldâ€aligned currents. Journal of Geophysical Research, 2009, 114, .	3.3	15
303	Wave telescope technique for MMS magnetometer. Geophysical Research Letters, 2016, 43, 4774-4780.	1.5	15
304	Automated forceâ€free flux rope identification. Journal of Geophysical Research: Space Physics, 2017, 122, 780-791.	0.8	15
305	Near-Earth plasma sheet boundary dynamics during substorm dipolarization. Earth, Planets and Space, 2017, 69, 129.	0.9	15
306	MESSENGER Observations of Rapid and Impulsive Magnetic Reconnection in Mercury's Magnetotail. Astrophysical Journal Letters, 2018, 860, L20.	3.0	15

#	Article	IF	CITATIONS
307	Dissipation of Earthward Propagating Flux Rope Through Reâ€reconnection with Geomagnetic Field: An MMS Case Study. Journal of Geophysical Research: Space Physics, 2019, 124, 7477-7493.	0.8	15
308	Formation of Macroscale Flux Transfer Events at Mercury. Astrophysical Journal Letters, 2020, 893, L18.	3.0	15
309	A Model for the Distant Tail Field: ISEE 3 Revisited. Journal of Geomagnetism and Geoelectricity, 1996, 48, 455-471.	0.8	15
310	Sources of fieldâ€aligned currents in the auroral plasma. Geophysical Research Letters, 1991, 18, 45-48.	1.5	14
311	Martian obstacle and bow shock: origins of boundaries anisotropy. Advances in Space Research, 2004, 33, 2222-2227.	1.2	14
312	Steepening of waves at the duskside magnetopause. Geophysical Research Letters, 2016, 43, 7373-7380.	1.5	14
313	Transport of Mass and Energy in Mercury's Plasma Sheet. Geophysical Research Letters, 2018, 45, 12,163.	1.5	14
314	Driftâ€Bounce Resonance Between Pc5 Pulsations and Ions at Multiple Energies in the Nightside Magnetosphere: Arase and MMS Observations. Geophysical Research Letters, 2018, 45, 7277-7286.	1.5	14
315	A Comparative Study of the Proton Properties of Magnetospheric Substorms at Earth and Mercury in the Near Magnetotail. Geophysical Research Letters, 2018, 45, 7933-7941.	1.5	14
316	A transient enhancement of Mercury's exosphere at extremely high altitudes inferred from pickup ions. Nature Communications, 2020, 11, 4350.	5.8	14
317	MESSENGER Observations of Mercury's Nightside Magnetosphere Under Extreme Solar Wind Conditions: Reconnectionâ€Generated Structures and Steady Convection. Journal of Geophysical Research: Space Physics, 2020, 125, e2019JA027490.	0.8	14
318	Polar cap potential distributions during periods of positive IMF By and Bz. Journal of Atmospheric and Solar-Terrestrial Physics, 1994, 56, 209-221.	0.9	13
319	Evolution of the plasmoid-lobe interaction with downtail distance. Geophysical Research Letters, 1994, 21, 2765-2768.	1.5	13
320	Energetic (>0.2 MeV) electron bursts in the deep geomagnetic tail observed by the Goddard Space Flight Center experiment on ISEE 3: Association with geomagnetic substorms. Journal of Geophysical Research, 1996, 101, 2723-2740.	3.3	13
321	A statistical study of the magnetic field structure in the inner magnetosphere. Journal of Geophysical Research, 1997, 102, 17571-17582.	3.3	13
322	Temporal relationship between midtail traveling compression regions and substorm onset: Evidence for near-Earth neutral line formation in the late growth phase. Journal of Geophysical Research, 1998, 103, 26607-26612.	3.3	13
323	Magnetosphere–Exosphere–Surface Coupling at Mercury. Space Science Reviews, 2007, 132, 551-573.	3.7	13
324	Flux transfer events simultaneously observed by Polar and Cluster: Flux rope in the subsolar region and flux tube addition to the polar cusp. Journal of Geophysical Research, 2008, 113, .	3.3	13

#	Article	IF	CITATIONS
325	Alfven Wave Reflection model of field-aligned currents at Mercury. Icarus, 2010, 209, 40-45.	1.1	13
326	The current system associated with the boundary of plasma bubbles. Geophysical Research Letters, 2014, 41, 8169-8175.	1.5	13
327	Coherent wave activity in Mercury's magnetosheath. Journal of Geophysical Research: Space Physics, 2015, 120, 7342-7356.	0.8	13
328	MESSENGER observations of the dayside lowâ€latitude boundary layer in Mercury's magnetosphere. Journal of Geophysical Research: Space Physics, 2015, 120, 8387-8400.	0.8	13
329	MESSENGER Observations of Flow Braking and Flux Pileup of Dipolarizations in Mercury's Magnetotail: Evidence for Current Wedge Formation. Journal of Geophysical Research: Space Physics, 2020, 125, e2020JA028112.	0.8	13
330	MAVEN Survey of Magnetic Flux Rope Properties in the Martian lonosphere: Comparison With Three Types of Formation Mechanisms. Geophysical Research Letters, 2021, 48, e2021GL093296.	1.5	13
331	Evidence of the influence of equatorial martian crustal magnetization on the position of the planetary magnetotail boundary by phobos 2 data. Advances in Space Research, 2001, 28, 885-889.	1.2	12
332	Unusually Distant Bow Shock Encounters at Mars: Analysis of March 24, 1989 event. Space Science Reviews, 2004, 111, 233-243.	3.7	12
333	Bow Shock and Upstream Phenomena at Mars. Space Sciences Series of ISSI, 2004, , 115-181.	0.0	12
334	Observational evidence of ring current in the magnetosphere of Mercury. Nature Communications, 2022, 13, 924.	5.8	12
335	The effect of solar wind structure on magnetospheric energy supply during solar cycle 20. Journal of Geophysical Research, 1981, 86, 675-680.	3.3	11
336	DE 1 observations of return current regions in the nightside auroral oval. Journal of Geophysical Research, 1988, 93, 14542-14548.	3.3	11
337	Cluster observation of continuous reconnection at dayside magnetopause in the vicinity of cusp. Annales Geophysicae, 2005, 23, 2199-2215.	0.6	11
338	Ionâ€scale structure in Mercury's magnetopause reconnection diffusion region. Geophysical Research Letters, 2016, 43, 5935-5942.	1.5	11
339	Proton Properties in Mercury's Magnetotail: A Statistical Study. Geophysical Research Letters, 2020, 47, e2020GL088075.	1.5	11
340	Processes influencing the diurnal variation of the <i>AL</i> index and its reliability. Journal of Geophysical Research, 1981, 86, 8977-8980.	3.3	10
341	Highly structured ionospheric convection for northward interplanetary magnetic field: A case study with DE 2 observations. Journal of Geophysical Research, 1995, 100, 14743.	3.3	10
342	Structure, force balance, and topology of Earth's magnetopause. Science, 2017, 356, 960-963.	6.0	10

#	Article	IF	CITATIONS
343	Modeling Study of the Geospace System Response to the Solar Wind Dynamic Pressure Enhancement on 17 March 2015. Journal of Geophysical Research: Space Physics, 2018, 123, 2974-2989.	0.8	10
344	Effects of Orbital Eccentricity and IMF Cone Angle on the Dimensions of Mercury's Magnetosphere. Astrophysical Journal, 2020, 892, 2.	1.6	10
345	Flux Transfer Events at a Reconnection‣uppressed Magnetopause: Cassini Observations at Saturn. Journal of Geophysical Research: Space Physics, 2021, 126, e2020JA028786.	0.8	10
346	Solar Wind-Magnetosphere Coupling and the Distant Magnetotail: ISEE-3 Observations. Astrophysics and Space Science Library, 1986, , 717-730.	1.0	10
347	, Particle-in-cell Simulations of Secondary Magnetic Islands: Ion-scale Flux Ropes and Plasmoids. Astrophysical Journal, 2020, 900, 145.	1.6	10
348	Field and thermal plasma observations of ULF pulsations during a magnetically disturbed interval. Journal of Geophysical Research, 1992, 97, 14859-14875.	3.3	9
349	Localized injection of large-amplitude Pc 1 waves and electron temperature enhancement near the plasmapause observed by DE 2 in the upper ionosphere. Journal of Geophysical Research, 1994, 99, 6187.	3.3	9
350	Modeling the response of the induced magnetosphere of Venus to changing IMF direction using MESSENGER and Venus Express observations. Geophysical Research Letters, 2009, 36, .	1.5	9
351	Stepwise tailward retreat of magnetic reconnection: THEMIS observations of an auroral substorm. Journal of Geophysical Research: Space Physics, 2016, 121, 4548-4568.	0.8	9
352	The Influence of IMF Clock Angle on Dayside Flux Transfer Events at Mercury. Geophysical Research Letters, 2017, 44, 10,829.	1.5	9
353	A Statistical Study of the Force Balance and Structure in the Flux Ropes in Mercury's Magnetotail. Journal of Geophysical Research: Space Physics, 2019, 124, 5143-5157.	0.8	9
354	Upstream Ultra‣ow Frequency Waves Observed by MESSENGER's Magnetometer: Implications for Particle Acceleration at Mercury's Bow Shock. Geophysical Research Letters, 2020, 47, e2020GL087350.	1.5	9
355	Photoionization Loss of Mercury's Sodium Exosphere: Seasonal Observations by MESSENGER and the THEMIS Telescope. Geophysical Research Letters, 2021, 48, e2021GL092980.	1.5	9
356	IMF <i>B</i> _{<i>y</i>} effects on ground magnetometer response to increased solar wind dynamic pressure derived from global MHD simulations. Journal of Geophysical Research: Space Physics, 2017, 122, 5028-5042.	0.8	9
357	, Reply [to "Comment on â€~An evaluation of three predictors of geomagnetic activity' by R. E. Holzer and J A. Slavinâ€]. Journal of Geophysical Research, 1983, 88, 4955-4958.	* 3.3	8
358	Energetic (>0.2 MeV) electron bursts observed by ISEE 3 in the deep (<240 <i>R_E</i>) geomagnetic tail. Journal of Geophysical Research, 1993, 98, 13441-13451.	3.3	8
359	Fine structure of low-energy H+in the nightside auroral region. Journal of Geophysical Research, 1994, 99, 4131.	3.3	8
360	The relationship between the magnetic field in the Martian magnetotail and upstream solar wind parameters. Journal of Geophysical Research, 1994, 99, 17199.	3.3	8

#	Article	IF	CITATIONS
361	Coordinated polar spacecraft, geosynchronous spacecraft, and ground-based observations of magnetopause processes and their coupling to the ionosphere. Annales Geophysicae, 2004, 22, 4329-4350.	0.6	8
362	Bow shock observations by Prognoz–Prognoz 11 data: analysis and model comparison. Advances in Space Research, 2005, 36, 1958-1963.	1.2	8
363	Flux closure during a substorm observed by Cluster, Double Star, IMAGE FUV, SuperDARN, and Greenland magnetometers. Annales Geophysicae, 2006, 24, 751-767.	0.6	8
364	Space Technology 5 measurements of auroral fieldâ€aligned current sheet motion. Geophysical Research Letters, 2009, 36, .	1.5	8
365	Saturation of the electric field transmitted to the magnetosphere. Journal of Geophysical Research, 2010, 115, .	3.3	8
366	Mercury's Dynamic Magnetosphere. , 2018, , 461-496.		8
367	Largeâ€Amplitude Oscillatory Motion of Mercury's Crossâ€Tail Current Sheet. Journal of Geophysical Research: Space Physics, 2020, 125, e2020JA027783.	0.8	8
368	The Magnetometer Instrument on MESSENGER. , 2007, , 417-450.		8
369	An Eastward Current Encircling Mercury. Geophysical Research Letters, 2022, 49, .	1.5	8
370	On the origin of reverse polarity TCRs. Geophysical Research Letters, 2001, 28, 1925-1928.	1.5	7
371	THE VELOCITY DISTRIBUTION OF PICKUP He ⁺ MEASURED AT 0.3 AU BY <i>MESSENGER</i> . Astrophysical Journal, 2014, 788, 124.	1.6	7
372	Evaluating Single Spacecraft Observations of Planetary Magnetotails With Simple Monte Carlo Simulations: 2. Magnetic Flux Rope Signature Selection Effects. Journal of Geophysical Research: Space Physics, 2018, 123, 10124-10138.	0.8	7
373	Structure and Configuration of Mercury's Magnetosphere. , 2018, , 430-460.		7
374	Cross‣cale Quantification of Stormâ€Time Dayside Magnetospheric Magnetic Flux Content. Journal of Geophysical Research: Space Physics, 2020, 125, e2020JA028027.	0.8	7
375	Dayside auroral particle acceleration mechanisms derived from dynamics explorer data Journal of Geomagnetism and Geoelectricity, 1990, 42, 1365-1378.	0.8	7
376	MESSENGER Observations of Planetary Ion Enhancements at Mercury's Northern Magnetospheric Cusp During Flux Transfer Event Showers. Journal of Geophysical Research: Space Physics, 2022, 127, .	0.8	7
377	Space Technology 5 multipoint observations of transpolar arc-related field-aligned currents. Journal of Geophysical Research, 2011, 116, n/a-n/a.	3.3	6
378	Solar Cycle Occurrence of Alfvénic Fluctuations and Related Geoâ€Efficiency. Journal of Geophysical Research: Space Physics, 2017, 122, 9848-9857.	0.8	6

#	Article	IF	CITATIONS
379	Dynamics Explorer Measurements of Particles, Fields, and Plasma Drifts Over a Horse-Collar Auroral Pattern Journal of Geomagnetism and Geoelectricity, 1992, 44, 1225-1237.	0.8	6
380	Empirical Relationships Between Interplanetary Conditions, Magnetospheric Flux Transfer, and the Al Index. Geophysical Monograph Series, 0, , 423-435.	0.1	5
381	A largeâ€scale view of Space Technology 5 magnetometer response to solar wind drivers. Earth and Space Science, 2015, 2, 115-124.	1.1	5
382	Evaluating Single‧pacecraft Observations of Planetary Magnetotails With Simple Monte Carlo Simulations: 1. Spatial Distributions of the Neutral Line. Journal of Geophysical Research: Space Physics, 2018, 123, 10109-10123.	0.8	5
383	MESSENGER Observations of Giant Plasmoids in Mercury's Magnetotail. Astrophysical Journal Letters, 2019, 886, L32.	3.0	5
384	Energetic (>0.2 MeV) Electron Bursts in the Deep Geomagnetic Tail Observed by ISEE 3: Association with Substorms and Magnetotail Structures. Journal of Geomagnetism and Geoelectricity, 1996, 48, 657-673.	0.8	5
385	DE-2 observations of filamentary currents at ionospheric altitudes. Geophysical Monograph Series, 1990, , 591-598.	0.1	4
386	Magnetotail currents during the growth phase and local auroral breakup. Geophysical Monograph Series, 2000, , 81-89.	0.1	4
387	Correlation between ground-based observations of substorm signatures and magnetotail dynamics. Annales Geophysicae, 2005, 23, 997-1011.	0.6	4
388	Traveling Compressions Regions. Geophysical Monograph Series, 0, , 225-240.	0.1	4
389	MESSENGER at Mercury: Early orbital operations. Acta Astronautica, 2014, 93, 509-515.	1.7	4
390	Response of reverse convection to fast IMF transitions. Journal of Geophysical Research: Space Physics, 2015, 120, 4020-4037.	0.8	4
391	Response of the Geospace System to the Solar Wind Dynamic Pressure Decrease on 11 June 2017: Numerical Models and Observations. Journal of Geophysical Research: Space Physics, 2019, 124, 2613-2627.	0.8	4
392	ARTEMIS Science Objectives. , 2011, , 27-59.		4
393	The solar probe mission. AIP Conference Proceedings, 1990, , .	0.3	3
394	Modeling ionospheric convection during a major geomagnetic storm on October 22-23, 1981. Journal of Geophysical Research, 1994, 99, 11017.	3.3	3
395	Evidence of different magnetotail responses to small solar wind pressure pulses depending on IMF Bz polarity. Geophysical Research Letters, 2001, 28, 4163-4166.	1.5	3
396	Magnetotail flows can consume as much solar wind energy as a substorm. Journal of Geophysical Research, 2003, 108, .	3.3	3

#	Article	IF	CITATIONS
397	Ionospheric signatures during a magnetospheric flux rope event. Annales Geophysicae, 2008, 26, 3967-3977.	0.6	3
398	The Earth: Plasma Sources, Losses, and Transport Processes. Space Sciences Series of ISSI, 2016, , 145-208.	0.0	3
399	Juno Observations of Ionâ€Inertial Scale Flux Ropes in the Jovian Magnetotail. Geophysical Research Letters, 2021, 48, e2020GL089721.	1.5	3
400	Physicsâ€Based Analytical Model of the Planetary Bow Shock Position and Shape. Journal of Geophysical Research: Space Physics, 2021, 126, e2021JA029104.	0.8	3
401	MESSENGER: Exploring Mercury's Magnetosphere. , 2007, , 133-160.		3
402	Hermean Magnetosphere-Solar Wind Interaction. Space Sciences Series of ISSI, 2008, , 347-368.	0.0	3
403	Examining the Magnetic Geometry of Magnetic Flux Ropes from the View of Single-point Analysis. Astrophysical Journal, 2020, 903, 53.	1.6	3
404	Properties of Ionâ€Inertial Scale Plasmoids Observed by the Juno Spacecraft in the Jovian Magnetotail. Journal of Geophysical Research: Space Physics, 2022, 127, .	0.8	3
405	MMS Observations of Field Line Resonances Under Disturbed Solar Wind Conditions. Journal of Geophysical Research: Space Physics, 2021, 126, e2020JA028936.	0.8	2
406	A 3D MHDâ€Particle Tracing Model of Na ⁺ Energization on Mercury's Dayside. Journal of Geophysical Research: Space Physics, 2021, 126, e2021JA029587.	0.8	2
407	The Magnetic Field of Mercury. Space Sciences Series of ISSI, 2009, , 307-339.	0.0	2
408	The cause of two plasma-tail disconnection events in comet P/Halley during the ICE-Halley radial period. , 1988, , 267-275.		2
409	Neptune's Pole-on Magnetosphere: Dayside Reconnection Observations by Voyager 2. Planetary Science Journal, 2022, 3, 76.	1.5	2
410	Dayside magnetopause reconnection and flux transfer events under radial interplanetary magnetic field (IMF): BepiColombo Earth-flyby observations. Annales Geophysicae, 2022, 40, 217-229.	0.6	2
411	Ionospheric signature of the tail neutral line during the growth phase of a substorm. Journal of Geophysical Research, 1996, 101, 5067-5073.	3.3	1
412	Unusually Distant Bow Shock Encounters at Mars: Analysis of March 24, 1989 Event. Space Sciences Series of ISSI, 2004, , 233-243.	0.0	1
413	Reactions to APS support of ERA. Physics Today, 1979, 32, 11-82.	0.3	0
414	Robert E. Holzer: In celebration of his 80th birthday. History of Geophysics, 1990, , 267-270.	0.0	0

#	Article	IF	CITATIONS
415	The Mercury dual orbiter mission. AIP Conference Proceedings, 1990, , .	0.3	0
416	Tomographic imaging of electron distributions: Leveraging computing power advances to produce inexpensive, low-power, lightweight, and robust instrumentation. Review of Scientific Instruments, 2003, 74, 1002-1007.	0.6	0
417	A Dynamic Twist in the Tail. Science, 2012, 336, 548-549.	6.0	0
418	Electric and Magnetic Field Fluctuations at High Latitudes in the Dayside Ionosphere During Southward IMF. Geophysical Monograph Series, 0, , 387-397.	0.1	0
419	Observations of upstream ultra-low-frequency waves in the Mercury's foreshock. , 2014, , .		0
420	Challenges in Measuring External Currents Driven by the Solar Wind-Magnetosphere Interaction. Terrestrial, Atmospheric and Oceanic Sciences, 2015, 26, 11.	0.3	0
421	Magnetosphere–Exosphere–Surface Coupling at Mercury. Space Sciences Series of ISSI, 2008, , 369-391.	0.0	0
422	A Review of General Physical and Chemical Processes Related to Plasma Sources and Losses for Solar System Magnetospheres. Space Sciences Series of ISSI, 2016, , 27-89.	0.0	0
423	Plasma Sources in Planetary Magnetospheres: Mercury. Space Sciences Series of ISSI, 2016, , 91-144.	0.0	0
424	A 3-D computational model for solar wind/magnetosphere interactions - Prediction of polar flattening of Jupiter and Saturn magnetospheres. , 1987, , .		0
425	Characteristics of the Martian Magnetosphere according to the Data of the Mars 3 and Phobos 2 Satellites: Comparison with MGS and MAVEN Results. Cosmic Research, 2021, 59, 478-492.	0.2	0
426	Energetic Ions Downtail of the Reconnection Site. Journal of Geophysical Research: Space Physics, 2022, 127, .	0.8	0